Molecular Biology of the Cell
Vol. 14, 2689–2705, July 2003

Transcytotic Efflux from Early Endosomes Is Dependent on Cholesterol and Glycosphingolipids in Polarized Hepatic Cells

Lydia K. Nyasae, Ann L. Hubbard,* and Pamela L. Tuma†

Department of Cell Biology, Johns Hopkins University School of Medicine, Baltimore, Maryland 21205

Submitted December 12, 2002; Revised March 3, 2003; Accepted March 13, 2003
Monitoring Editor: Jennifer Lippincott-Schwartz

We examined the role that lipid rafts play in regulating apical protein trafficking in polarized hepatic cells. Rafts are postulated to form in the *trans*-Golgi network where they recruit newly synthesized apical residents and mediate their direct transport to the apical plasma membrane. In hepatocytes, single transmembrane and glycolipid-anchored apical proteins take the "indirect" route. They are transported from the *trans*-Golgi to the basolateral plasma membrane where they are endocytosed and transcytosed to the apical surface. Do rafts sort hepatic apical proteins along this circuitous pathway? We took two approaches to answer this question. First, we determined the detergent solubility of selected apical proteins and where in the biosynthetic pathway insolubility was acquired. Second, we used pharmacological agents to deplete raft components and assessed their effects on basolateral-to-apical transcytosis. We found that cholesterol and glycosphingolipids are required for delivery from basolateral early endosomes to the subapical compartment. In contrast, fluid phase uptake and clathrin-mediated internalization of recycling receptors were only mildly impaired. Apical protein solubility did not correlate with raft depletion or impaired transcytosis, suggesting other factors contribute to apical protein insolubility. Examination of apical proteins in Fao cells also revealed that raft-dependent sorting does not require the polarized cell context.

INTRODUCTION

The plasma membrane (PM) of polarized epithelial cells is physically continuous, but functionally and compositionally divided into two separate domains: the apical and basolateral. The molecular sorting mechanisms and pathways by which newly synthesized PM proteins achieve their specific yet asymmetric distributions are actively being examined in many polarized epithelial cell types. One important question is how domain-specific, integral PM proteins find their way into the right intracellular path. In general, structural signals, such as amino acid sequences, conformations or modifications on the protein itself, are thought to specify the cellular destination. Several such signals required for basolateral PM targeting and/or localization have been identified, and generally they reside in the cytoplasmic tails of the proteins (reviewed in Ikonen and Simons, 1998; Gu *et al.*, 2001; Tuma and Hubbard, 2001). Most of the signals contain either a tyrosine in the context of a short degenerate sequence or a dileucine motif. Some signals overlap with those used at the PM in receptor-mediated endocytosis, whereas other basolateral signals, such as that in the polymeric IgA receptor (pIgA-R), are unique.

The identification of cytoplasmic signals that mediate apical PM targeting has been much more elusive. Many apical residents (e.g., single transmembrane domain [TMD] ectoenzymes) have very short cytoplasmic tails (6–8 amino acids) or lack them entirely (e.g., glycophoshatidylinositol [GPI]-anchored proteins). However, two apical sorting signals have been proposed: extracellular glycans on the apical residents or the incorporation of apical residents into specialized membrane domains (Scheiffele *et al.*, 1995; Harder and Simons, 1997). The latter sorting mechanism is the focus of this study.

Article published online ahead of print. Mol. Biol. Cell 10.1091/mbc.E02–12–0816. Article and publication date are available at www.molbiolcell.org/cgi/doi/10.1091/mbc.E02–12–0816.

* Corresponding author. E-mail address: alh@jhmi.edu.
† Present address: Department of Biology, The Catholic University of America, Washington, DC.

Abbreviations used: APN, aminopeptidase N; ASGP-R, asialoglycoprotein receptor; DPP IV, dipeptidyl peptidase IV; FB1, fumonisin B1; GPI, glycophoshatidylinositol; LPDM, lipoprotein deficient medium; mβCD, methyl-β-cyclodextrin; 5′NT, 5′nucleotidase; pIgA-R, polymeric IgA receptor; PM, plasma membrane; SAC, subapical compartment; SM, sphingomyelin; TLC; thin layer chromatography; Tf-R, transferrin receptor; TMD; transmembrane domain.

© 2003 by The American Society for Cell Biology

The "raft hypothesis" for apical protein sorting emerged from two fundamental observations. First, glycosphingolipids and cholesterol are enriched in the apical surfaces of epithelial cells. The intrinsic properties of these lipid species are thought to promote their assembly into specialized membrane domains called "rafts" (for review, see Harder and Simons, 1997; Brown and London, 1998). Second, selected proteins are recruited to these domains based on their biophysical properties. In particular, GPI-anchored proteins, which are predominantly expressed at the apical PM, are found in rafts. Thus, according to the raft hypothesis for protein sorting, rafts form in the biosynthetic pathway where they recruit apically destined proteins (especially GPI-anchored proteins), and then they with their recruited cargo are transported in vesicles directly to the apical domain.

Do lipid rafts sort apical residents in polarized hepatocytes? Unlike most simple polarized epithelial cells, the predominant route to the hepatic apical PM is indirect. Newly synthesized apical proteins are delivered from the *trans*-Golgi network (TGN) first to the basolateral PM where they are selectively internalized and transcytosed to the apical surface. Are apical proteins sorted into rafts at the TGN for delivery to the basolateral PM? Once delivered to the basolateral PM, are apical proteins recruited into rafts that are necessary for apical targeting along the transcytotic route? If so, are rafts present at the basolateral domain or in other transcytotic intermediates?

We determined that only a subset of apical residents in polarized WIF-B cells was detergent insoluble. Examination of the acquisition of insolubility of newly synthesized proteins indicated that apical residents become insoluble with different kinetics and at different places along the biosynthetic pathway. In cholesterol or glycosphingolipid-depleted cells, the basolateral-to-apical transcytosis of all apical residents examined and pIgA-R was inhibited. Apical proteins were basolaterally internalized, but blocked at early endosomes, indicating that rafts are required for endosomal transcytotic efflux. Biochemical and morphological examination of apical proteins in Fao cells further revealed that raft-dependent sorting is conserved in nonpolarized cells.

MATERIALS AND METHODS

Reagents and Antibodies

trans-[^{35}S]Methionine was purchased from ICN Biomedicals (Irvine, CA). Triton X-100, protein A-Sepharose, F12 (Coon's modification) medium, lipoprotein deficient serum (LPDM), methyl-β-cyclodextrin (mβCD), cholesterol-loaded mβCD, fumonisin B1 (FB1), horseradish peroxidase (HRP) (type VI), and cytochalasin D were purchased from Sigma-Aldrich (St. Louis, MO). Latrunculin B was purchased from BIOMOL Research Laboratories (Plymouth Meeting, PA). Lovastatin was from A.G. Scientific (San Diego, CA). HRP-conjugated secondary antibodies and Super Signal West Pico chemiluminescence substrate were from Amersham Biosciences (Piscataway, NJ) and Pierce Chemical (Rockford, IL), respectively. Alexa-conjugated secondary antibodies were from Molecular Probes (Eugene, OR). Anti-transferrin receptor (Tf-R) antibodies were purchased from Accurate Chemical & Scientific (Westbury, NY) and anti-V5 epitope tag antibodies were from Invitrogen (Carlsbad, CA). Anti-5′nucleotidase (5′NT) (monoclonal and affinity purified polyclonal), -CD59 (affinity-purified monoclonals), and -Tf-R (polyclonal) were kindly provided by J.P. Luzio (Cambridge University, Cambridge, United Kingdom), P. Morgan (University of Wales College of Medicine, Cardiff, United Kingdom), and M. Farquhar (University of California, San Diego, San Diego, CA), respectively. Antibodies against aminopeptidase N (APN), asialoglycoprotein receptor (ASGP-R), CE9, pIgA-R, dipeptidylpeptidase IV (DPP IV), and HA321 were prepared in the Hubbard laboratory and have been described previously (Bartles *et al.*, 1985; Hubbard *et al.*, 1985; Barr and Hubbard, 1993; Ihrke *et al.*, 1993; Shanks *et al.*, 1994).

Cell Culture

WIF-B and Fao cells were grown in a humidified 7% CO_2 incubator at 37°C as described previously (Ihrke *et al.*, 1993; Shanks *et al.*, 1994). Briefly, cells were grown in F-12 medium (Coon's modification), pH 7.0, supplemented with 5% fetal bovine serum. WIF-B medium was also supplemented with 10 μM hypoxanthine, 40 nM aminoterpin, and 1.6 μM thymidine. In general, cells were seeded onto glass coverslips at 1.3×10^4 cells/cm^2. Fao cells were cultured for 3–5 d and WIF-B cells for 8–12 d until they reached maximum density and polarity.

Exogenous Expression of DPP IV and pIgA-R

WIF-B or Fao cells were infected with recombinant adenovirus particles ($0.7–1.4 \times 10^{10}$ virus particles/ml) encoding V5/His6 epitope-tagged full-length DPP IV or pIgA-R for 30 min at 37°C as described previously (see Bastaki *et al.*, 2002 for detailed methods and description of constructs). The cells were washed with complete medium and incubated an additional 18 h to allow expression.

Immunoblot Analysis

Cells were rinsed in cold phosphate-buffered saline (PBS) and extracted for 30 min on ice in 0.15 ml of lysis buffer [1% (vol/vol) Triton X-100, 150 mM NaCl, 25 mM HEPES, pH 7.4] containing 1 μg/ml each of aprotinin, pepstatin, antipain, leupeptin, benzamidine, and phenylmethylsulfonyl fluoride. The samples were sheared using a 26-gauge needle and centrifuged at $120{,}000 \times g$ for 30 min at 4°C. The resultant pellet was resuspended to volume with SDS-PAGE sample buffer and boiled for 3 min. Reducing sample buffer was used for analysis of all proteins except HA321 and CD59 both of which required nonreducing conditions (lacking β-mercaptoethanol) for optimal immunodetection. For immunoblotting, anti-5′NT (affinity purified polyclonal) was diluted to 1:200, anti-CE9, pIgAR and -Tf-R (rabbit polyclonal sera) were diluted 1:5000, whereas ASGP-R and APN polyclonal sera were diluted to 1:1000 and 1:2000, respectively. Anti-CD59 (affinity purified monoclonal) was diluted to 1 μg/ml. HRP-conjugated secondary antibodies were used at 5 ng/ml, and immunoreactivity was detected with enhanced chemiluminescence. The relative levels of immunoreactive species in the soluble and insoluble fractions were determined by densitometric comparison of immunoreactive bands.

In Figure 3, cells were treated with 5 mM mβCD for the indicated times in medium prepared with 5% LPDM and extracted as described above. In Figure 5, cells were treated for 24 or 48 h in complete medium with 25 μM FB1 diluted in methanol. For the 48-h samples, cells were renewed with fresh medium and drug after the first 24 h. The control cells were treated with the same methanol concentration for 48 h, renewing after 24 h.

Metabolic Labeling

WIF-B cells were incubated in cysteine- and methionine-free medium for 1 h at 37°C. Cells were then labeled for 10 min at 37°C in the same medium containing 100–200 μCi of *trans*-[^{35}S]methionine. Cells were rinsed with Hanks' buffered saline solution, placed in prewarmed, complete medium containing excess unlabeled cysteine (64 μg/ml) and methionine (20 μg/ml) and chased at 37°C for the indicated times. For the 20°C block, cells were either first chased for 10 min at 37°C after labeling or transferred directly to precooled chase medium at 20°C for 2 h. To release the 20°C block, prewarmed

medium was added and the cells returned to 37°C. At the indicated times, the cells were rinsed with Hanks' buffered saline solution and once with cold PBS before extracting and immunoprecipitation.

Immunoprecipitations

APN and HA321. The detergent-soluble and -insoluble samples were prepared as described above for immunoblotting with a few modifications. The coverslips were instead solubilized in 0.9 ml of lysis buffer, centrifuged, and the resultant pellet solubilized in 0.2 ml of solubilization buffer (1% SDS, 50 mM Tris, 5 mM EDTA, pH 8.8), sheared with a 26-gauge needle until fully resuspended, and diluted to 1.0 ml with lysis buffer. The supernatants were corrected to contain the same concentration of solubilization buffer components and diluted to 1.0 ml with lysis buffer. The detergent-soluble and -insoluble samples were serially immunoprecipitated, first with anti-APN polyclonal antibodies (1:1000) at 4°C for 16 h. Protein A-Sepharose was added for 4 h and samples processed as described previously (Bartles *et al*., 1987). The samples were then incubated with affinity-purified polyclonal anti-HA321 (1:1000) and processed as for anti-APN immunoprecipitations. Immunoprecipitates were separated by SDS-PAGE and transferred to nitrocellulose. The membranes were exposed from 18 h to 4 d to phosphorimaging plates that were scanned using a PhosphorImager (Fuji, Tokyo, Japan).

5′NT. Cells were rinsed in cold PBS and lysed in parallel at 4°C for 30 min or at 37°C for 15 min in 0.9 ml of lysis buffer. The 4°C lysates were centrifuged at 120,000 × *g* for 30 min at 4°C and the 37°C lysates at 25°C. The supernatants were supplemented to contain 20 mM octylglucoside, 10 mM Tris, 1 mM EDTA and diluted to 1.0 ml with lysis buffer. Directly conjugated monoclonal antibody-Sepharose was used to immunoprecipitate 5′NT as described previously (Schell *et al*., 1992).

Thin Layer Chromatography (TLC)

Cholesterol was measured in control or treated cells grown on coverslips. At the indicated times, total lipids were extracted as described previously (Bligh and Dyer, 1959) and separated on 10 × 10 cm high-performance TLC plates with a mobile phase of hexane/ethyl acetate (80:20). To measure sphingomyelin (SM), control or FB1-treated cells were extracted as described previously (Bligh and Dyer, 1959) and the lipids separated with a mobile phase of chloroform/methanol/concentrated ammonia (20:5:0.5). Lipids were visualized by charring plates that had been sprayed with 3% cupric acetate (wt/vol) in 8% phosphoric acid (Macala *et al*., 1983).

Immunofluorescence Microscopy

Control or treated cells were fixed on ice with chilled PBS containing 4% PFA for 1 min and permeabilized with ice-cold methanol for 10 min. Cells were processed for indirect immunofluorescence as described previously (Ihrke *et al*., 1993). Alexa 488- or 568-conjugated secondary antibodies were used at 3–5 μg/ml.

Internalization Assays

Cholesterol-depleted Cells. WIF-B or Fao cells were pretreated for 5 min in LPDM in the absence or presence of 5 mM mβCD. Proteins present at the basolateral PM in WIF-B cells or the PM in Fao cells were continuously labeled with specific antibodies diluted in LPDM in the continued absence or presence of mβCD. Rabbit polyclonals against ASGP-R, APN, and DPP IV were diluted 1:100, 1:200, and 1:500, respectively. Mouse anti-5′NT, anti-V5, and anti-CD59 were diluted 1:1000, 1:2000, and 1:500, respectively, and hybridoma supernatant containing anti-TF-R antibodies was diluted 1:5. After labeling, cells were fixed as described above, and the trafficked antibodies were labeled with Alexa-488 or -568–conjugated secondary antibodies (3–5 μg/ml) as described previously (Ihrke *et al*., 1998).

For recovery assays, cells were pretreated in LPDM containing 5 mM mβCD for 60 min. Cells were rinsed twice in prewarmed LPDM and incubated an additional 60 min in LPDM in the absence or presence of 365 μg/ml cholesterol-loaded mβCD (equivalent to the addition of 20 μg/ml free cholesterol). Antigens at the basolateral PM (in WIF-B cells) or PM (in Fao cells) were continuously labeled for 60 min in the continued presence of the drug, fixed, permeabilized, and stained as described above.

Sphingolipid-depleted Cells. WIF-B cells were pretreated for 48 h in complete medium in the absence or presence of 25 μM FB1 (medium and drug renewed daily). For experiments where DPP IV or pIgA-R expression was required, cells were infected with recombinant adenovirus after the first day of FB1 treatment. Cells were antibody labeled, fixed, and stained as described above.

Kinetic Assays

Total IgG from serum (APN or DPP IV) or ascites (5′NT) were purified (EZ-Sep; Pharmacia AB, Uppsala, Sweden) and biotinylated (EZ-Link sulfo-NHS-biotin; Pierce Chemical) according to the manufacturers' instructions. To measure internalization, WIF-B cells were continuously labeled with biotinylated antibodies for the indicated times at 37°C. The remaining surface-associated antibodies were eluted with isoglycine (200 mM glycine, 150 mM NaCl, pH 2.5) for 5 min at room temperature and the cells lysed in isoglycine containing 20 mM octylglucoside and 0.5% Triton X-100 for 30 min on ice. Aliquots of the eluate and lysate were incubated in streptavidin-coated 96-well plates (Pierce Chemical). Bound antibodies were detected with HRP-conjugated secondary antibodies followed by colorimetric detection with an HRP substrate detection kit (Bio-Rad, Hercules, CA).

Recycling Assays

Fao PM proteins were continuously labeled as described for the internalization assays. To strip surface-associated antibodies, cells were incubated in isoglycine as described above. The cells were rinsed with PBS, placed in prewarmed LPDM in the absence or presence of 5 mM mβCD, and incubated at 37°C for 60 min. Cells were fixed and labeled as described for the internalization assays.

Imaging

Labeled cells were visualized by epifluorescence (Axioplan Universal microscope; Carl Zeiss, Jena, Germany). Images were acquired with a Princeton MicroMax cooled charge-coupled device camera (Roper Scientific, Trenton, NJ) and IP Labs software (Scanalytics, Fairfax, VA). Further image processing and figure compilation was performed using Photoshop (Adobe Systems, Mountain View, CA) and Microsoft PowerPoint software (Microsoft, Redmond, WA).

RESULTS

Only a Subset of Hepatic Apical Residents Are Detergent Insoluble

To determine the role that rafts play in regulating apical protein trafficking in polarized hepatic cells, we first examined the solubility properties of different classes of endogenously expressed apical residents in Triton X-100. We chose a high-speed centrifugation for separation of the soluble and insoluble fractions (see DISCUSSION). As reported for other epithelial cells, the GPI-anchored proteins that we examined

were virtually insoluble in 1% Triton X-100 at 4°C in WIF-B cells. As shown in Figure 1A, >85 and 95% of 5′NT and CD59, respectively, were detergent insoluble at steady state. Approximately 50% of APN, a single TMD apical resident, was also detergent insoluble. Conversely, two other single TMD apical proteins, DPP IV and pIgA-R, were completely soluble (Figure 1A). These differential solubility properties among the apical residents indicate that raft incorporation is not a prerequisite for apical PM distribution in hepatic cells. For comparison, we examined the solubility properties of several basolateral proteins. Basolateral residents, CE9 (Figure 1A) and HA321 (Figure 2), and basolateral recycling receptors, ASGP-R and Tf-R (Figure 1A), were entirely soluble in Triton X-100.

Incorporation into Rafts at the TGN Is Not Required for Apical PM Sorting of 5′NT

Because 5′NT, CD59, and APN were partially detergent insoluble, we determined where in their life cycles insolubility was acquired. The approach we chose was metabolic pulse labeling followed by extraction into soluble and insoluble pools and immunoprecipitation with specific antibodies. However, 5′NT recovered in the insoluble fraction could not be resolubilized for subsequent immunoprecipitation. Although APN was quantitatively recovered in immunoprecipitates from the pelleted fraction resuspended in solubilization buffer and boiled for 3 min (see MATERIALS AND METHODS and Figure 2), none of the >85% of insoluble 5′NT was recovered (Figure 1B). Changing the solubilization temperature or time also did not allow for 5′NT immunoprecipitation from this fraction (Figure 1B).

To overcome this experimental barrier, we adopted an alternative method (Cerneus *et al.*, 1993) for determining the insolubility of newly synthesized 5′NT. Unlike at 4°C, all of 5′NT was soluble in Triton X-100 at 37°C (Figure 1C). From the densitometric analysis of the Western blot shown, the steady-state amount of 5′NT recovered in the supernatant and pelleted fractions at 4°C was the same as that recovered in the supernatant at 37°C (160 versus 163 arbitrary density units). Furthermore, 5′NT in the 37°C extracts was quantitatively immunoprecipitated (Figure 1C). Thus, the proportion of insoluble 5′NT was determined by subtracting the amount of 5′NT immunoprecipitated from the 4°C soluble pool (the soluble fraction) from the amount recovered in the 37°C extracts (the total population) (Figure 1C). Using this method, we determined that 87.0 ± 6.6% of 5′NT is Triton X-100 insoluble, nearly identical to the value determined from steady state Western blotting (Figure 1A). Thus, this method was suitable for the subsequent metabolic labeling experiments.

Cells were ^{35}S-labeled for 10 min and then chased for 0–120 min at 37°C. At each time point, cells were extracted with 1% Triton X-100, the detergent-insoluble and -soluble pools prepared and the specific molecules immunoprecipitated. Mature APN reached steady-state insolubility levels (~45%) quickly, after only 30 min of chase (Figure 2a). Insoluble populations of mature 5′NT were also detected after 30-min chase, but accounted for only 20% of the total mature protein pool (Figure 2b). After 60 min of chase, when 5′NT molecules were fully mature, only ~50% of the 5′NT population was insoluble. Steady-state insolubility levels were not observed until 3–5 h of chase (our unpublished data), suggesting that apical delivery was required for complete insolubility to be achieved, a process that takes >4 h in intact hepatocytes (Schell *et al.*, 1992) or >3 h in WIF-B cells (Ihrke *et al.*, 1998). We also noticed that after the 10-min label (0-min chase), 25% of 5′NT was already mature, yet none of this population was insoluble. This suggested that insolubility might not be achieved until basolateral delivery (see below). For comparison, we examined the solubility properties of the newly synthesized basolateral resident, HA321 (Figure 2c). Like APN and 5′NT, mature forms of HA321 were detected after short chase periods, and by 60 min, the molecules were fully mature. HA321 was not detected in the insoluble fractions consistent with its steady-state solubility properties.

To determine whether the insolubility of APN and 5′NT was acquired in the TGN, the presumed site of raft formation (Simons and Ikonen, 1997), metabolically pulse-labeled cells were subjected to a 2-h 20°C temperature block before an additional chase at 37°C. The 20°C incubation produces a block in post-Golgi transport such that newly synthesized proteins accumulate in the Golgi (Matlin and Simons, 1983; Griffiths *et al.*, 1985; Saraste *et al.*, 1986; our unpublished data). Although only 30% of APN was detected in its mature form after the 2 h block (0 min after release), ~25% of that population was detected in an insoluble pool (Figure 2d). As more newly synthesized APN matured during the subsequent chase at 37°C, the proportion of insoluble APN remained constant, suggesting that APN acquired its insolubility in the TGN and maintained it thereafter. In contrast, 75% of ^{35}S-labeled 5′NT was mature after the temperature block (Figure 2e), but none was detected in an insoluble pool. To make sure that the 20°C block was not accumulating 5′NT in compartments preceding the TGN, cells were chased for 10 min at 37°C before imposing the 20°C block to allow further transit along the biosynthetic pathway. As before, nearly all of newly synthesized 5′NT was mature under these conditions, but no insoluble populations were detected (our unpublished data). HA321 examined under the same conditions was never detected in an insoluble pool (Figure 2f). These results indicated that different hepatic apical residents were incorporated into detergent-insoluble domains with differing kinetics and at different places along the biosynthetic pathway. A percentage of the single TMD protein, APN, was likely incorporated into rafts at the TGN, whereas the GPI-anchored protein, 5′NT, became raft-associated much later. These observations together with the finding that many apical PM proteins are completely detergent-soluble indicate that raft association is not a universal requirement for sorting apical residents from the TGN to the basolateral PM in polarized hepatic cells.

Transcytosis Is Cholesterol Dependent

To determine whether raft association was important in regulating transcytosis in hepatic cells, we depleted polarized WIF-B cells of cholesterol, a condition reported to dissociate raft components (Ohtani *et al.*, 1989; Kilsdonk *et al.*, 1995; Scheiffele *et al.*, 1997). As measured by TLC, cholesterol was rapidly depleted by the addition of 5 mM mβCD (Figure 3A). After only 15 min of treatment, cholesterol levels fell to 52.5 ± 6.4% of control, and by 60 min, were 23.0 ± 10.7% of control. To ensure that mβCD was not toxic when cholesterol was depleted to such low levels, we measured

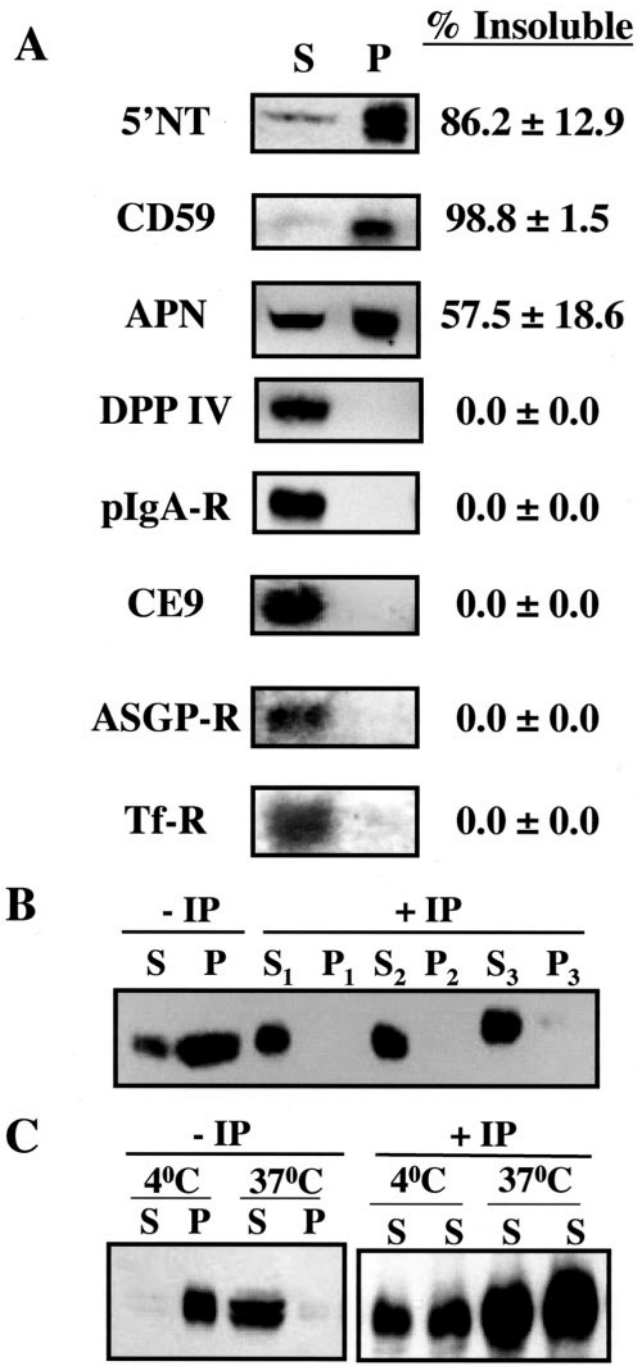

Figure 1. A subset of apical PM residents in polarized WIF-B cells is insoluble in Triton X-100. (A) WIF-B cells were extracted in 1% Triton X-100 at 4°C for 30 min and the soluble and insoluble fractions were separated by centrifugation. The soluble (S) and pelleted (P) fractions were analyzed by Western blotting with the indicated antibodies. The fraction of the total population that was detergent insoluble for each molecule is indicated on the right (% Insoluble). Values are expressed as the mean ± SD. Measurements were done on at least three experiments each performed in duplicate. (B) 5′NT steady-state distributions into the S and P fractions after Triton X-100 extraction are shown (−IP). The pelleted fraction was resuspended in solubilization buffer and the soluble fraction corrected for solubilization buffer components (see MATERIALS AND METHODS). The fractions were then incubated for 3 min at 100°C (S_1, P_1) or at room temperature for 30 min (S_2, P_2) or 60 min (S_3, P_3). The fractions were immunoprecipitated with 5′NT monoclonal antibodies and immunoblotted with 5′NT polyclonal antibodies (+IP). None of the 5′NT in the pelleted fractions was immunoprecipitated (compare P with P_1, P_2 or P_3). (C) WIF-B cells were extracted in 1% Triton X-100 for 30 min at 4 or 37°C and the soluble and insoluble fractions separated by centrifugation. The S and P fractions were analyzed by Western blotting with 5′NT antibodies (−IP). The resultant soluble fractions were immunoprecipitated with 5′NT monoclonal antibodies and immunoblotted with 5′NT polyclonal antibodies (+IP). Duplicate samples are shown. 5′NT was quantitatively immunoprecipitated from both the 4 and 37°C soluble fractions. Only 16% of the starting material was loaded in the −IP samples, whereas the total immunoprecipitation was analyzed in the +IP lanes.

cell viability by trypan blue exclusion. Cells incubated for 60 min in LPDM alone (control) or in the presence of 5 mM mβCD had similar viability levels (91.4 ± 1.9% of control and 89.7 ± 2.6% of treated). Moreover, cells remained polarized (our unpublished data). We also examined the effects of adding lovastatin, another commonly used cholesterol-depleting drug. However, even after 3 d of treatment in LPDM, cholesterol levels fell by only 20% (our unpublished data).

We next determined the solubility properties of apical proteins in cholesterol depleted WIF-B cells. In the presence of mβCD, only the solubility of APN was significantly altered. After 15 min of treatment, nearly all of this single TMD protein was detected in the soluble fraction (Figure 3, B and C). In contrast, only small percentages of 5′NT and CD59 (12 and 14%, respectively) were soluble after 60 min, a time point at which ~80% of the cholesterol was extracted (Figure 3, B and C).

We then determined whether cholesterol depletion impaired transcytosis of basolaterally located apical proteins. Cells were pretreated for 5 min with LPDM in the absence or presence of 5 mM mβCD. Transcytosis was monitored by continuously labeling the basolateral pool of selected apical proteins or recycling receptors in the absence or presence of mβCD for 60 min. The cells were fixed, permeabilized, and the trafficked antibody–antigen complexes visualized with secondary antibodies. Although cholesterol depletion did not change the steady-state apical protein distributions (our unpublished data), it severely impaired transcytosis of all apical molecules tested. As reported previously, control cells showed intense fluorescence labeling of all apical markers tested at the apical PM after 60 min (see Figure 4a for an example). This result indicated successful transcytotic delivery. In contrast, the apical domains in treated cells had no apparent fluorescence labeling for any apical resident tested, whereas a reciprocal increase in basolateral staining was often observed. CD59, APN, DPP IV, and pIgA-R trafficking are shown in Figure 4, b, c, e, and g, respectively. We also examined the trafficking of Tf-R and ASGP-R, recycling receptors that, like pIgA-R, are internalized by clathrin-mediated mechanisms. Surprisingly, both receptors were internalized in the same cells where a block in transcytosis of the apical residents was observed. Cotraf-

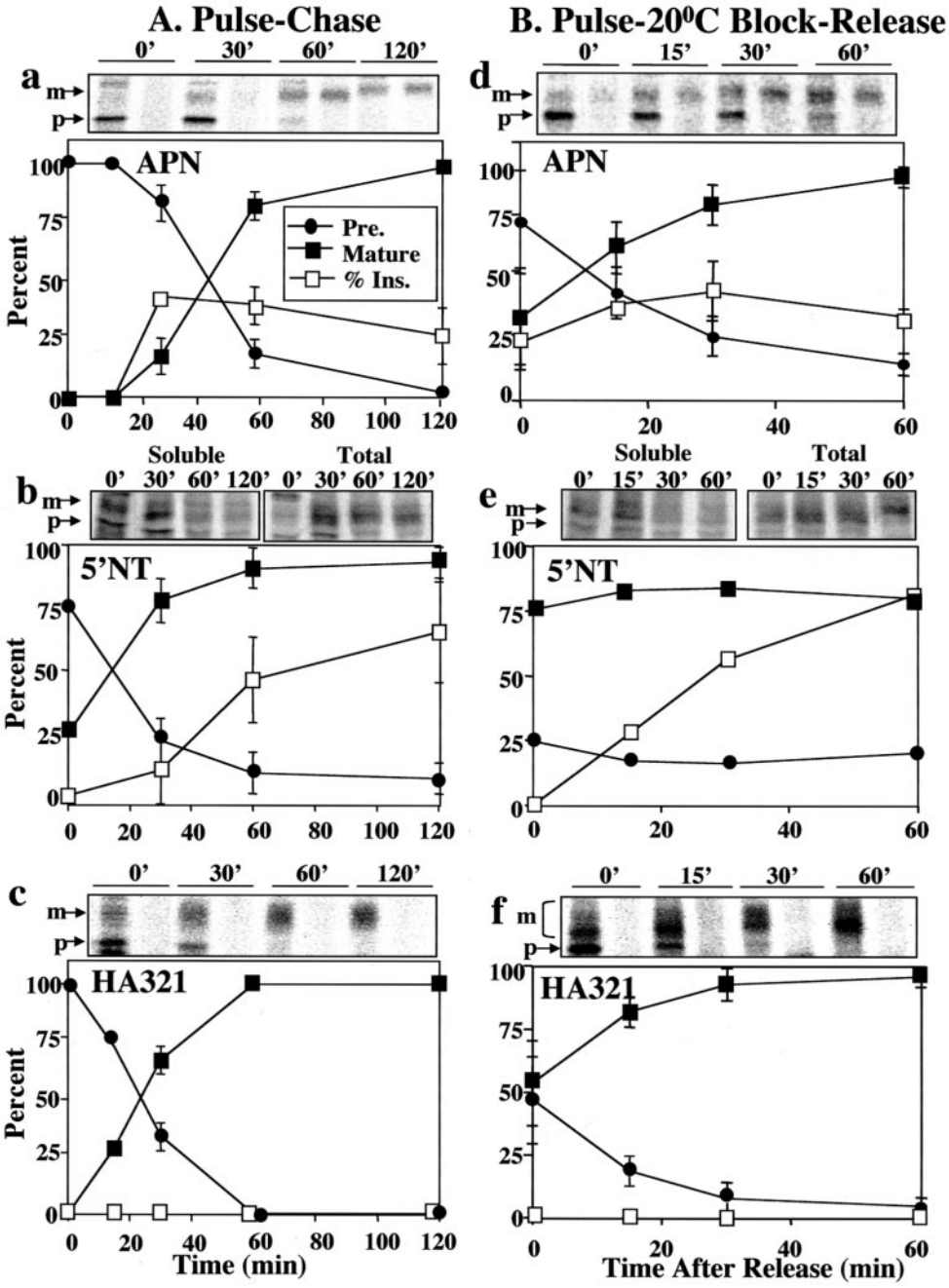

Figure 2. Apical residents acquire detergent insolubility with different kinetics and at different places in the biosynthetic pipeline. (A) WIF-B cells were pulse-labeled with ^{35}S-amino acids for 10 min and chased at 37°C for the indicated times. Cells were then extracted in 1% Triton X-100 for 30 min at 4°C or 15 min at 37°C and the soluble and insoluble fractions separated by centrifugation. Immunoprecipitations were performed on the fractions with the indicated antibodies and processed for autoradiography. Values are expressed as the mean ± SD. Measurements were done on at least three experiments each performed in duplicate. Autoradiographs from representative experiments are shown. For each time point in a and c, the soluble (left lane) and insoluble (right lane) fractions are shown. In b, the immunoprecipitates from extracts performed at 4°C (soluble) and 37°C (total) are shown. Arrows are pointing to the precursor (p) and mature (m) forms of the newly synthesized proteins. (B) WIF-B cells were pulse-labeled with ^{35}S-amino acids for 10 min at 37°C. After washing, cells were incubated for 2 h at 20°C to accumulate newly synthesized proteins in the Golgi. The 20°C medium was replaced with medium prewarmed to 37°C and the labeled proteins chased for the indicated times at 37°C. Samples were processed as described in A. Values in d and f are expressed as the mean ± SD and were obtained from measurements done on at least three experiments each performed in duplicate. In e, values are averages of measurements obtained from two experiments, both performed in duplicate. Representative autoradiographs as described in A are shown.

ficking of APN and Tf-R is shown in Figure 4, c and d, whereas DPP IV or pIgA-R cotrafficking with ASGP-R is shown in Figure 4, e and f, and g and h, respectively. The robust internalization of the fluid phase marker HRP was also observed in control and mβCD-treated cells (our unpublished data). Although virtually no apical labeling was observed for DPP IV, intracellular labeling was observed that colocalized with ASGP-R (Figure 4, e and f, insets; see below).

The exogenous addition of cholesterol reversed the mβCD-induced defect in transcytosis. Cells were first treated for 60 min with mβCD, which impaired transcytosis (Figure 4i), and then the drug was removed and the cells incubated for 60 min in LPDM containing 365 μg/ml cholesterol-loaded mβCD. Cells were subsequently labeled with anti-APN antibodies for an additional hour in the continued presence of the agent. As shown in Figure 4j, APN staining was detected at the apical PM with a concomitant decrease in basolateral PM staining, indicating reversal of the mβCD-induced impairment. No such recovery was observed in cells that did not receive exogenous cholesterol (our unpublished data). Thus, the defect

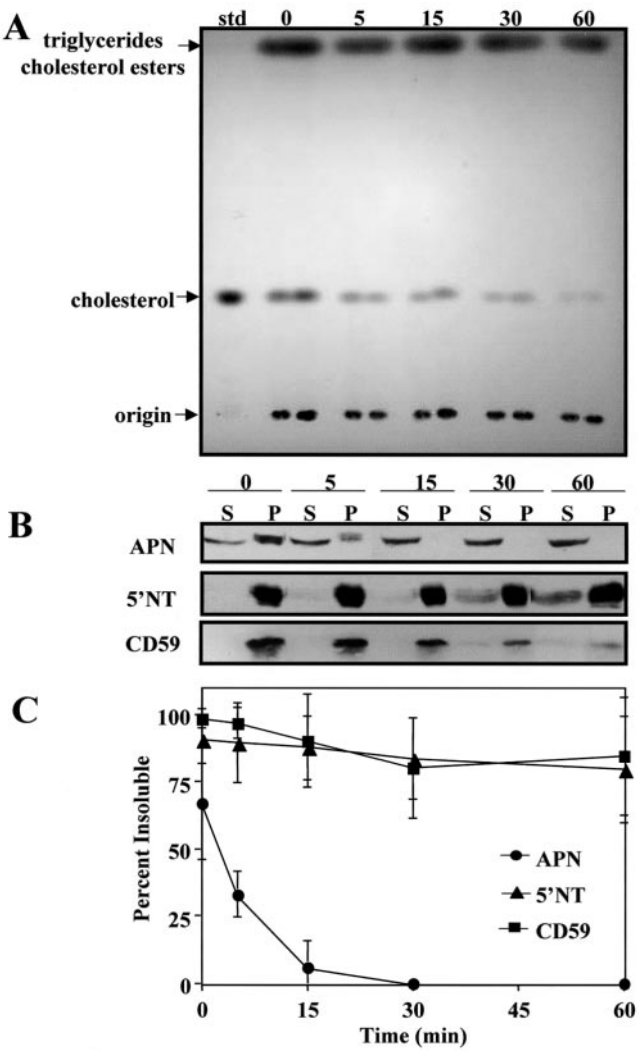

Figure 3. Cholesterol is rapidly depleted in WIF-B cells treated with mβCD, but the GPI-anchored apical residents remain detergent insoluble. (A) WIF-B cells were treated for the indicated times (in minutes) in LPDM containing 5 mM mβCD. Total lipids were extracted, separated by TLC and visualized by charring. Duplicate samples for each time point are shown. (B) Coverslips processed in parallel to those in A were extracted in 1% Triton X-100 for 30 min on ice and the soluble and insoluble fractions were separated by centrifugation. The soluble (S) and pelleted (P) fractions were analyzed by Western blotting with the indicated antibodies. (C) The relative levels of immunoreactive species in the soluble and insoluble fractions as shown in B were determined by densitometric comparison of immunoreactive bands, and the values for the insoluble populations are plotted. Values are expressed as the mean ± SD. Measurements were done on at least three experiments each performed in duplicate. std, cholesterol standard.

in transcytosis was likely due to cholesterol depletion directly.

We quantitated the morphological observations shown in Figure 4 by measuring the relative fluorescence intensity present at the apical and basolateral surfaces of 100–300 individual cells (Table 1). In control cells, the ratio of apical-to-basolateral fluorescence for all markers tested was >1, indicating that higher levels of fluorescence labeling was detected at the apical PM. Notably, the ratios for 5′NT and pIgA-R were higher than the others, likely reflecting their faster transcytosis kinetics (Ihrke *et al.*, 1998). In contrast, the ratios of apical-to-basolateral PM staining in treated cells were all <1 and represented decreases from 70 to 90% relative to control cells (values in parentheses). This reciprocal staining is evident in Figure 4. These results indicate that cholesterol is required for transcytosis of single TMD and GPI-anchored apical residents, even though it seems not to be relevant to their detergent solubility properties.

Transcytosis Is Glycosphingolipid Dependent

We next determined whether depletion of glycosphingolipids, other raft components, also impaired transcytosis. We treated cells with 25 μM FB1 and monitored glycosphingolipid depletion by measuring SM levels by TLC. Although SM levels do not specifically reflect cellular gylcosphingolipid levels, FB1 inhibits the formation of a common biosynthetic precursor. Also, SM is far more abundant than specific glycosphingolipids in WIF-B cells, allowing for more accurate TLC measurement. After 24 h in FB1, ~40% of the SM pool was depleted, and by 48 h, >60% was depleted (Figure 5A). These TLC conditions also resolved cholesterol and as indicated by the arrow in Figure 5A, its levels were unchanged by FB1 treatment. The detergent solubility of 5′NT, CD59, and APN were not altered by FB1 treatment alone (Figure 5B), although addition of *both* FB1 and mβCD solubilized APN and CD59, but only ~ 50% of 5′NT (Figure 5C). We also examined the effect of two actin-depolymerizing agents, cytochalasin D and latrunculin B, alone and in combination with lipid-depleting agents on apical protein insolubility. None of the three apical residents were released into a high-speed detergent supernatant after the agents were used alone. When both mβCD and cytochalasin D were added, APN and CD59 were mostly solubilized, but 5′NT remained in the pelleted fraction. Together, these results indicate that other factors impart detergent insolubility to 5′NT.

Although no changes in the solubility properties of the apical residents were observed after 48 h of FB1 treatment, transcytosis of all apical proteins tested was significantly impaired. The bright apical labeling of 5′NT in control cells (Figure 6a) was clearly absent from cells treated with FB1 (Figure 6b). Apical delivery of APN, DPP IV, and pIgA-R was also significantly decreased (Figure 6, c, e, and g). Our quantitative analysis (Table 1) confirmed these observations and further revealed that the FB1-induced block on transcytosis was less severe than that caused by cholesterol depletion. In all cases, the ratio of apical-to-basolateral fluorescence was greater in FB1-treated cells than in mβCD-treated cells. The overall decreased severity likely reflects the incomplete depletion of glycosphingolipids by FB1. In contrast, internalization of ASGP-R and Tf-R seemed to be more similar to that in control cells. Cotrafficking of APN and Tf-R is shown in Figure 6, c and d, and DPP IV or pIgA-R with ASGP-R in Figure 6, e and f, and g and h, respectively. Although little apical labeling by DPP IV or pIgA-R was observed, intracellular labeling was detected that colocalized with ASGP-R (Figure 6, e–h, insets; see below).

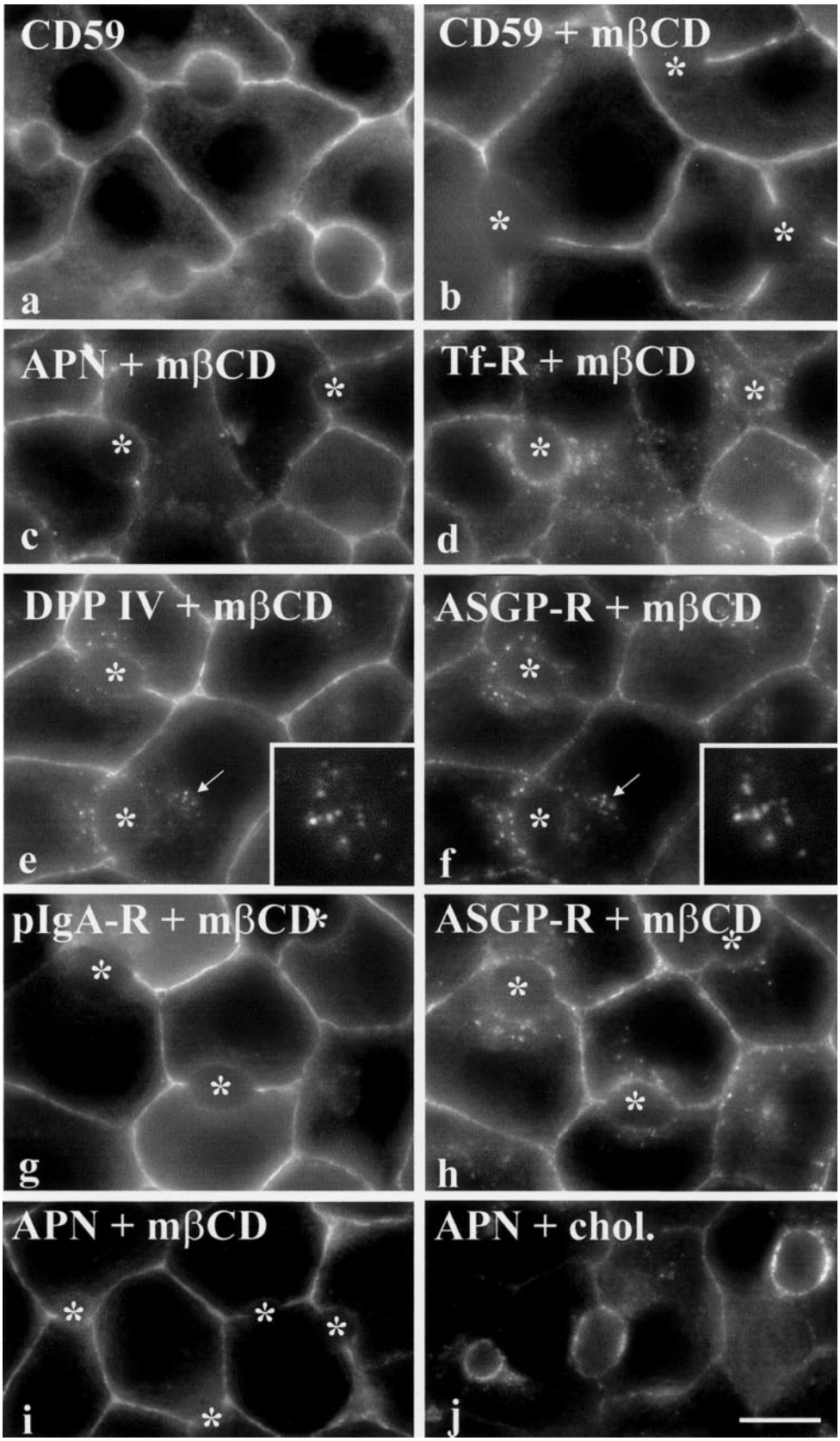

Figure 4. Transcytosis of newly synthesized apical residents is dramatically impaired by cholesterol depletion. WIF-B cells were pretreated for 5 min in LPDM in the absence (a) or presence of 5 mM mβCD (b–i). The indicated apical residents or recycling receptors present at the basolateral PM were continuously labeled with specific antibodies for 60 min at 37°C. The cells were fixed, permeabilized, and the trafficked antibody–antigen complexes visualized with secondary antibodies. In j, the medium containing mβCD was removed, the cells were rinsed in LPDM and then reincubated in LPDM containing 365 μg/ml cholesterol-loaded mβCD for 60 min at 37°C. APN was continuously antibody labeled for 60 min in the presence of the mβCD-cholesterol (chol). The cells were fixed, permeabilized, and the trafficked antibody–antigen complexes visualized with secondary antibodies. Asterisks are marking bile canaliculi (BC). Arrows in e and f are pointing to intracellular puncta enlarged in the insets approximately twofold. Bar, 10 μm.

Table 1. mβCD and FB1 impair apical protein trafficking in WIF-B and Fao cells

	Apical/Basolateral PM Fluorescence WIF-B Cells			Intracellular/PM Fluorescence Fao Cells	
Molecule	Control	+ mβCD	+ FB1	Control	+ mβCD
5′NT	4.16 ± 0.97	0.68 ± 0.10 (84)	0.76 ± 0.05 (82)	2.11 ± 0.21	0.21 ± 0.03 (90)
CD59	1.10 ± 0.22	0.28 ± 0.01 (75)	0.41 ± 0.13 (63)	ND	ND
APN	3.71 ± 1.30	0.34 ± 0.07 (91)	0.66 ± 0.14 (82)	1.58 ± 0.29	0.20 ± 0.06 (87)
DPP IV	1.71 ± 0.24	0.51 ± 0.06 (70)	0.78 ± 0.19 (54)	1.39 ± 0.49	0.39 ± 0.02 (72)
pIgA-R	5.99 ± 2.44	0.59 ± 0.07 (90)	1.43 ± 0.06 (76)	7.43 ± 1.78	2.37 ± 1.01 (68)

Apical proteins present at the basolateral PM in WIF-B cells or at the PM in Fao cells were continuously labeled for 60 min at 37°C in the absence or presence of either agent. Cells were fixed and permeabilized, and the trafficked antibodies were labeled with fluorescently conjugated secondary antibodies (see MATERIALS AND METHODS for details). Random fields were visualized by epifluorescence and digitized. From micrographs, the average pixel intensity of selected regions of interest (ROIs) placed at the apical or basolateral PM of the same WIF-B cell or at the intracellular apical compartment or PM of the same Fao cell was measured using the Measure ROI tool of the IP Labs imaging software. In general, the ROI area was 30–50 pixels^2, and multiple ROIs were collected in the same cell to verify that representative intensities were measured. The averaged background pixel intensity was subtracted from each value, and the ratio of apical PM to basolateral PM (WIF-B) or intracellular to PM (Fao) fluorescence intensity was determined. The percentage of inhibition for each condition is shown in parentheses. Approximately 100–300 cells were measured for each condition. Values are expressed as the mean ± S.D.

Apical Proteins Are Basolaterally Internalized in Cholesterol- and Glycosphingolipid-depleted Cells

To further characterize the block imposed by raft disruption in WIF-B cells, we determined the step in the transcytotic pathway that was impaired by mβCD or FB1 treatment. First, we examined whether the block was occurring at the basolateral PM by measuring internalization of basolaterally labeled apical proteins in control and treated cells. As shown in Figure 7A, the internalization of 5′NT was only minimally impaired (<20%) by mβCD, and only after 60 min of treatment. This minor impairment does not account for the >80% decrease in apical delivery observed (Table 1). Likewise, the impairment of APN internalization by mβCD (~35%), albeit greater than that seen for 5′NT, could not account for the >90% decrease in APN apical delivery (Table 1). Furthermore, DPP IV basolateral internalization was virtually unaffected by mβCD; after 60 min of treatment, internalization levels were 97% of control (our unpublished data). Thus, cholesterol depletion does not significantly block internalization from the basolateral PM in WIF-B cells.

Consistent with the biochemical results, we detected intracellular labeling of transcytosing apical proteins in both control and lipid-depleted cells. However, the extent that the intracellular apical proteins colocalized with recycling receptors in the two conditions was very different. In control cells, the transcytosing proteins colocalized in juxta-apical structures. As shown in Figure 7B, a and b, nearly perfect colocalization was observed for the single TMD protein, APN, and the GPI-anchored protein, 5′NT. These structures represent the supapical compartment (SAC), the previously identified transcytotic intermediate, because they largely excluded cotrafficked ASGP-R, which recycles between early endosomes and the PM (Figure 7B, e and f) (Wall and Hubbard, 1985; Ihrke *et al.*, 1998; Tuma and Hubbard, 2001). Although apical proteins traverse the early endosome in control cells, the absence of significant colocalization of ASGP-R and the apical proteins suggests that the latter quickly traverse this compartment. Similarly, the transcytosing apical residents and Tf-R that traverses the early endosome en route to the recycling endosome were not observed in the same intracellular puncta (Figure 7B, i and j). In contrast, ASGP-R and Tf-R were partially colocalized in control cells (Figure 7B, m and n). These puncta likely represent the early endosome, a common intermediate in the cellular itineraries of both receptors.

Similar to control cells, substantial overlap of apical proteins in intracellular structures was observed in mβCD-treated cells (Figure 7B, c and d), but these puncta were larger and contained ASGP-R (Figure 7B, g and h, and see Figure 4, e and f). The ASGP-R–positive puncta also partially overlapped with Tf-R (Figure 7B, k and l), and unlike for control cells, the Tf-R-positive puncta also contained transcytosing pIgA-R (Figure 7B, o and p). Similar staining patterns were observed in FB1-treated cells (our unpublished data; Figure 6, e and f). Thus, proteins that normally have different final destinations were found in the same structures after lipid depletion. The simplest interpretation is that mβCD and FB1 block transcytotic efflux from basolateral early endosomes, common trafficking intermediates of apical residents and recycling receptors.

Cholesterol Depletion Impairs Apical Protein Trafficking in Nonpolarized Hepatic Fao Cells

We have recently shown that apical proteins are selectively internalized from the nonpolarized PM of Fao cells, delivered to a novel compartment containing only other apical

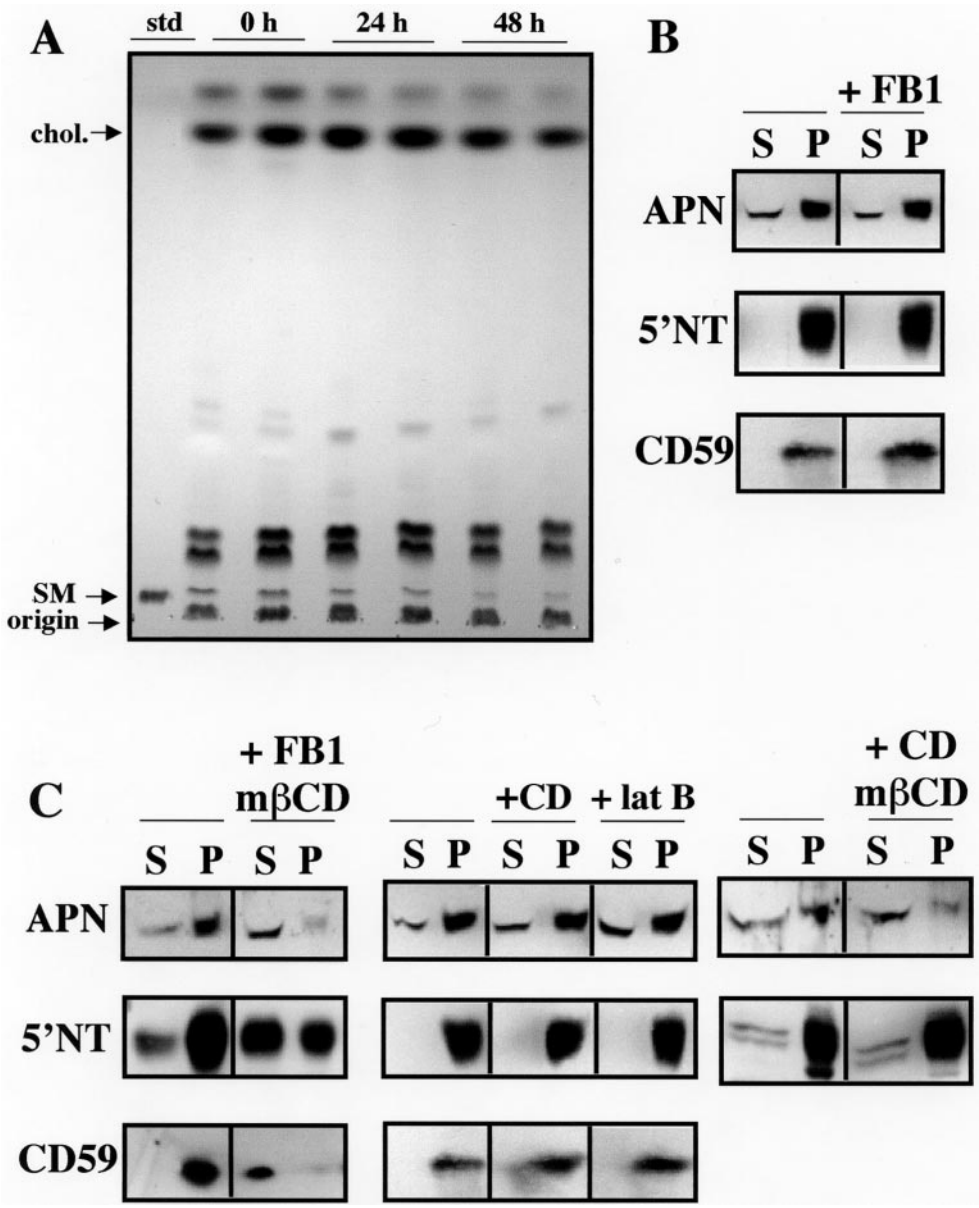

Figure 5. Glycosphingolipids are depleted in WIF-B cells treated with FB1, but the solubility properties of the apical residents do not change. (A) WIF-B cells were treated for the indicated times in medium containing 25 μM FB1. Total lipids were extracted, separated by TLC and visualized by charring. Duplicate samples for each time point are shown. (B) WIF-B cells were treated for 48 h in the absence or presence of FB1, extracted in 1% Triton X-100 at 4°C for 30 min and the soluble and insoluble fractions were separated by centrifugation. The soluble (S) and pelleted (P) fractions were analyzed by Western blotting with the indicated antibodies. (C) In the left-hand panels, WIF-B cells were treated with LPDM containing 5 mM mβCD and 25 μM FB1. The mβCD was added in the final hour of the 48-h FB1 treatment. In the middle panels, cells were treated with 10 μM cytochalasin D (CD) or latranculin B (lat B) for 60 min and in the right hand panels, cells were treated in LPDM containing both cytochalasin D and mβCD. Detergent extractions and sample processing were performed as described in B. Representative TLC and Western blotting results from three independent experiments are shown. std, standard; chol., cholesterol.

proteins and rapidly recycled back to the PM (Tuma *et al.*, 2002). Are the solubility properties of apical proteins and the cholesterol dependence of apical protein trafficking shared by nonpolarized cells or do they depend on the polarized cell context? To answer this question, we examined apical proteins in nonpolarized hepatic Fao cells biochemically and morphologically.

The solubility properties of the different classes of apical proteins in Fao cells were strikingly similar to those observed in polarized WIF-B cells. Both of the GPI-anchored proteins were virtually insoluble in Triton X-100, whereas APN was ~50% insoluble (Figure 8A). As in polarized cells, CE9, Tf-R and ASGP-R were entirely soluble (our unpublished data). Interestingly, ~25% of DPP IV was insoluble in Fao cells, which may reflect its much higher endogenous concentration than in WIF-B cells (Shanks *et al.*, 1994; our unpublished data). In fact, when overexpressed in WIF-B cells, ~25% of DPP IV was insoluble (our unpublished data; see DISCUSSION). These results suggest the presence of an apical domain is not required for the steady-state insolubility properties of apical proteins. Also striking is the finding that the solubility properties of these proteins were altered similarly by mβCD (Figure 8A). CD59 and 5′NT were solubilized ~ 8–11% in Fao cells compared with 12–14% in WIF-B cells, whereas APN was completely solubilized in both cell types.

Unlike for WIF-B cells, mβCD treatment changed the steady-state distributions of the apical proteins in Fao cells. In control cells, all apical proteins we have examined reside at the PM and in a novel, intracellular compartment (Tuma *et al.*, 2002). An example of this staining pattern is shown in

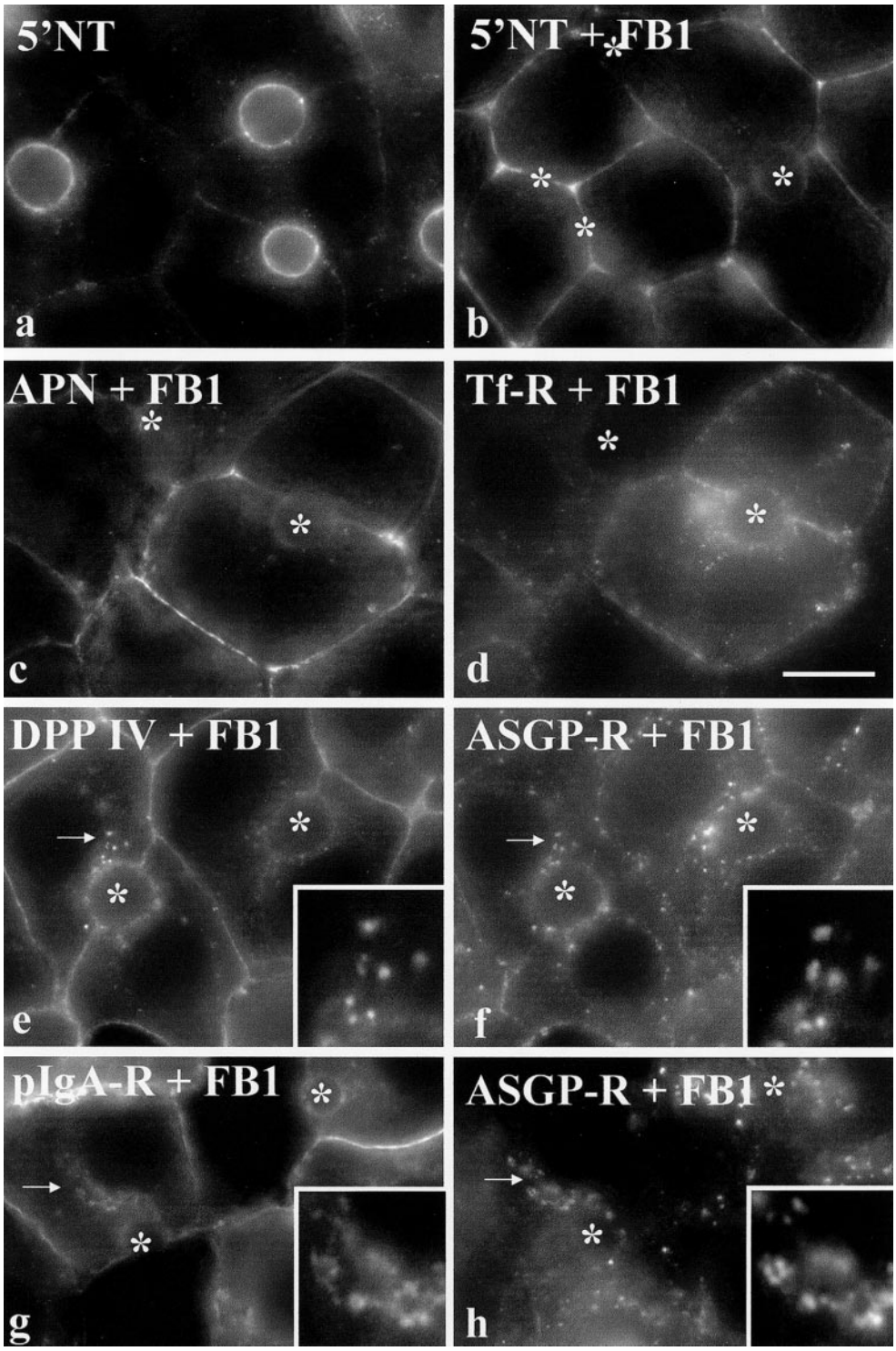

Figure 6. Transcytosis of newly synthesized apical residents is impaired by glycosphingolipid depletion. WIF-B cells were pretreated for 48 h in the absence (a) or presence of 25 μM FB1 (b–h). The indicated apical residents or recycling receptors present at the basolateral PM were continuously labeled with specific antibodies for 60 min at 37°C. The cells were fixed, permeabilized and the trafficked antibody–antigen complexes visualized with secondary antibodies. Asterisks are marking bile canaliculi (BC). Arrows in e–h are pointing to intracellular puncta enlarged in the insets approximately twofold. Bar, 10 μm.

Figure 8B, a. After mβCD treatment, no intracellular labeling of 5′NT was present and a reciprocal increase in PM staining was observed (Figure 8B, b). To determine whether the loss of intracellular staining reflected impaired apical protein internalization or recycling, we monitored the trafficking of surface-labeled apical proteins in control and treated cells. In control cells, transport to the intracellular compartment was readily detectable after 60 min of labeling (Figure 8C, a). However, in the presence of mβCD, no intracellular labeling of any apical protein tested was observed. 5′NT, APN, and

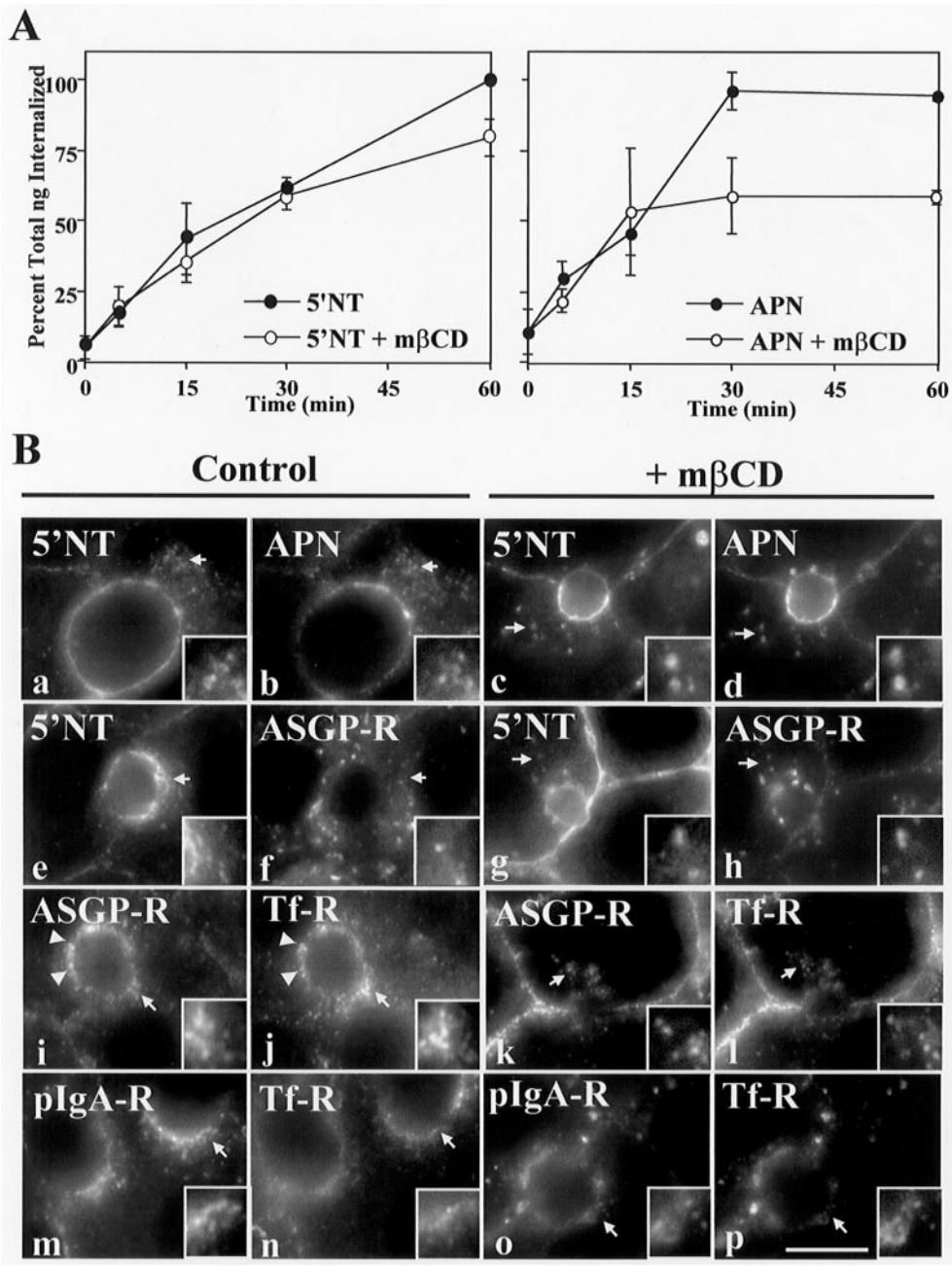

Figure 7. Apical residents are internalized in mβCD-treated cells and found in early endosomes. (A) To measure internalization, WIF-B cells were continuously labeled with biotinylated antibodies diluted in LPDM in the absence or presence of 5 mM mβCD for the indicated times at 37°C. The remaining PM-associated antibodies were eluted with isoglycine for 5 min at room temperature and the cells lysed. Aliquots of the eluate and lysate (the internalized population) were assayed for amounts of biotinylated antibodies using streptavidin-coated 96-well plates and colorimetric detection of HRP-conjugated secondary antibodies. The total amount (in nanograms) of antibody internalized is plotted relative to the maximum observed at 60 min in control cells, which was set to 100%. Values are expressed as the mean ± SD. Measurements were done on at least three experiments each performed in duplicate. (B) WIF-B cells were pretreated for 5 min in LPDM in the absence (a, b, e, f, i, j, m, and n) or presence of 5 mM mβCD (c, d, g, h, k, l, o, and p). The indicated apical residents or recycling receptors present at the basolateral PM were continuously labeled with specific antibodies for 60 min at 37°C. The cells were fixed, permeabilized, and the trafficked antibody–antigen complexes visualized with secondary antibodies. Arrows are pointing to intracellular clusters enlarged in the insets approximately twofold. In c, d, g, and o, images were intentionally overexposed to highlight the intracellular population of the transcytosing proteins. Thus, the apparent apical labeling is exaggerated. The insets in m and n are highlighting a region where Tf-R and ASGP-R do not significantly overlap. Arrowheads are pointing to colocalized structures. Bar, 10 μm.

DPP IV trafficking are shown in Figures 8C, b, c, and e, respectively. As in polarized WIF-B cells, we found that both ASGP-R and Tf-R were internalized in the same cells in which apical protein trafficking was blocked. Cotrafficking of APN and Tf-R and of DPP IV and ASGP-R is shown in Figures 8C, c and d, and e and f, respectively. Quantitation of these results is shown in Table 1. In this case, the intracellular fluorescence intensity was measured relative to the intensity present at the PM of the same cell. The apical compartment to PM ratios were all >1 in control cells, whereas in treated cells, the ratios were drastically reduced (~70–90%). Thus, cholesterol depletion impaired trafficking to the apical compartment in nonpolarized cells. Addition of exogenous cholesterol reversed the trafficking defect; 5′NT trafficking to the intracellular compartment returned in the presence of 365 μg/ml cholesterol-loaded mβCD (Figure 9, a and b).

To determine whether recycling from the apical compartment was also impaired, we examined the trafficking of staged apical proteins. Antibody-labeled APN was continuously internalized for 60 min to load the intracellular compartment (Figure 9c). Residual antibodies were surface stripped using isoglycine (Figure 9d). Recycling to the PM

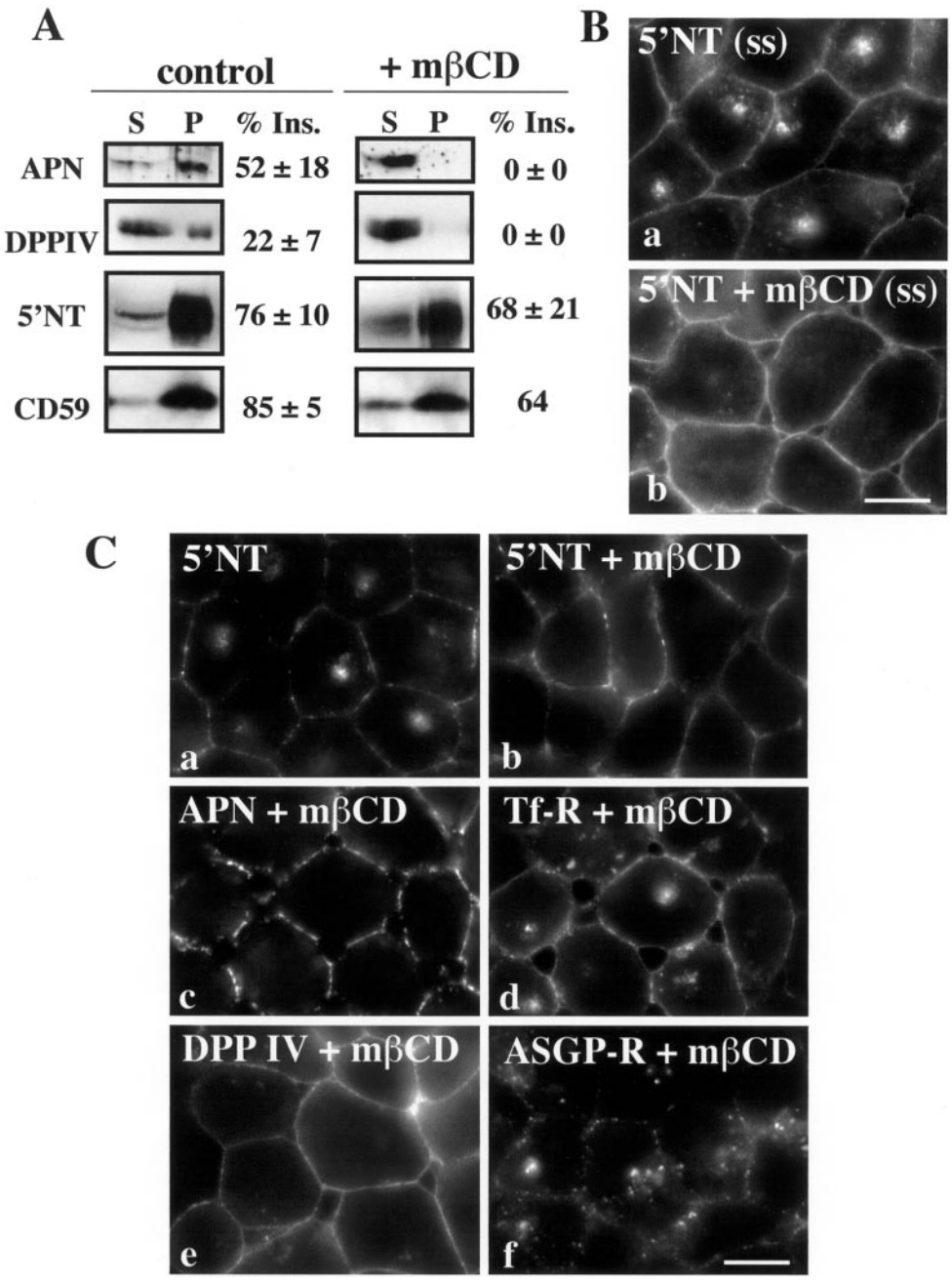

Figure 8. Cholesterol depletion impairs apical protein trafficking in nonpolarized hepatic Fao cells. (A) Fao cells were treated with LPDM in the absence (control) or presence of 5 mM mβCD for 60 min at 37°C. Cells were extracted in 1% Triton X-100 for 30 min and the soluble and insoluble fractions separated by centrifugation. The soluble (S) and pelleted (P) fractions were analyzed by Western blotting with the indicated antibodies. The fraction of the total population that was detergent insoluble for each molecule is indicated on the right (% Ins.). (B) Fao cells were treated in LPDM in the absence or presence of 5 mM mβCD as indicated. The steady-state (ss) distributions of 5′NT are shown. In C, the indicated apical residents or recycling receptors present at the PM were continuously labeled with specific antibodies for 60 min at 37°C. The cells were fixed, permeabilized, and the trafficked antibody–antigen complexes visualized with secondary antibodies. In general, the treated Fao cells seemed to have altered cell-to-cell adhesion, resulting in the formation of gaps between adjacent cells, which are not to be confused with the BC present in polarized WIF-B cells. Bar, 10 μm.

was monitored in the absence (Figure 9e) or presence of mβCD (Figure 9f). In both cases, PM fluorescence was regained indicating that recycling does not require cholesterol.

DISCUSSION

Cholesterol and Glycosphingolipids Are Specifically Required for Transcytotic Efflux from Early Endosomes

The trafficking of apical proteins, recycling receptors, and HRP in control and treated WIF-B cells is summarized in Figure 10. In control cells, newly synthesized apical proteins are sorted from the TGN to the basolateral PM where they are selectively internalized and transcytosed to the apical surface (Bartles *et al*., 1987; Bartles and Hubbard, 1988; Schell *et al*., 1992; Ihrke *et al*., 1998). Only two intermediates in the hepatic basolateral-to-apical transcytotic pathway have been identified: the basolateral early endosome and SAC (Barr *et al*., 1995; Ihrke *et al*., 1998). The early endosome also serves as a trafficking intermediate in at least four separate pathways. One is recycling, where internalized proteins are returned directly to the basolateral PM (e.g., ASGP-R; Wall and Hub-

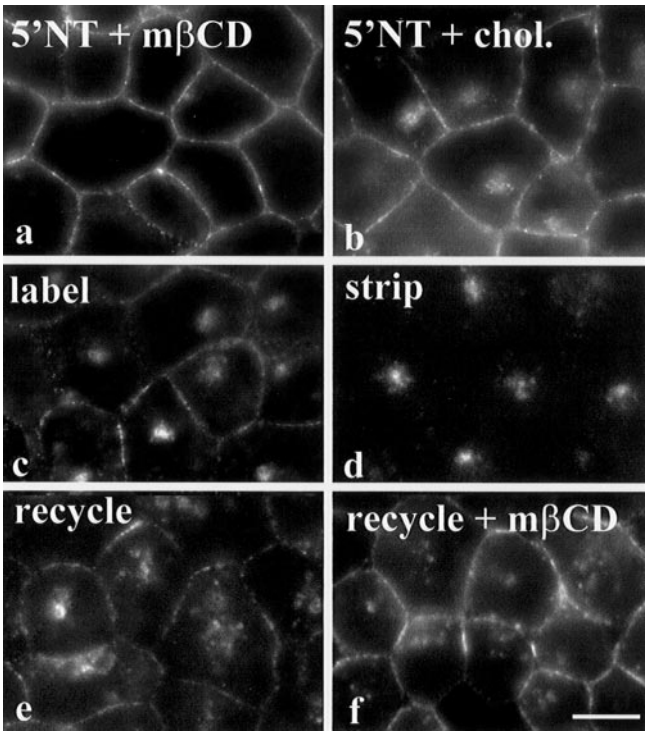

Figure 9. The mβCD defect is reversible and cholesterol depletion does not impair recycling in nonpolarized Fao cells. The cells in a and b were assayed for recovery as described in the legend to Figure 4. In c, APN present at the PM was continuously antibody-labeled for 60 min at 37°C. The remaining PM-associated antibodies were stripped with isoglycine for 5 min at room temperature (d). Only the protected, internalized APN–antibody complexes were detected. Cells were incubated an additional hour at 37°C in the absence (e) or presence (f) of 5 mM mβCD. The cells were fixed, permeabilized, and the antibody–antigen complexes visualized with secondary antibodies. Bar, 10 μm.

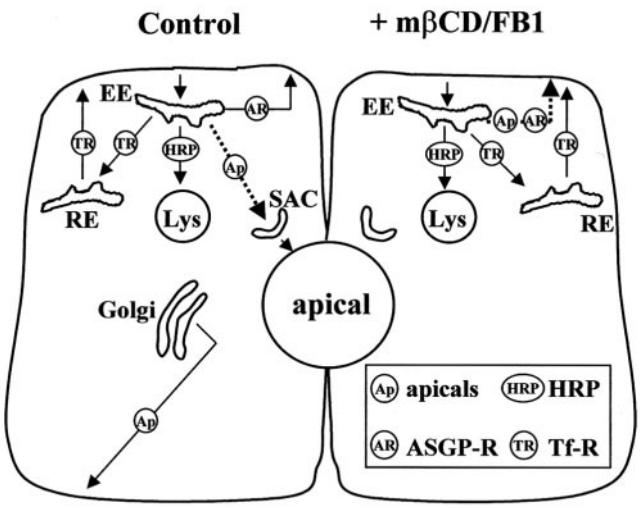

Figure 10. Intracellular itineraries of apical proteins in control and lipid-depleted WIF-B cells. In control cells, newly synthesized apical proteins are delivered from the TGN to the basolateral PM. They are selectively retrieved by endocytosis and transcytosed to the apical PM. Only two intermediates in the basolateral-to-apical transcytotic pathway have been identified: the basolateral early endosome and SAC. In treated cells, Golgi-to-basolateral PM delivery is unchanged and transcytosing proteins are internalized from the basolateral PM and delivered to the early endosome. Transport from the early endosome to the SAC is inhibited, and we propose that the apical residents recycle back to the basolateral PM. Except for the transcytotic efflux from the compartment, all other pathways are largely unaffected by cholesterol or glycosphingolipid depletion. EE, early endosome; Lys, lysosome; RE, recycling endosome.

bard, 1985). Another is endocytic targeting to lysosomes represented by HRP. A third pathway is transport to recycling endosomes depicted by Tf-R, and fourth is the transcytotic pathway that is taken by apical residents. At present, it is not known whether internalized apical proteins normally recycle between the early endosome and basolateral PM. Also, except for pIgA-R, the mechanisms that mediate basolateral internalization of apical residents are not known.

In mβCD- or FB1-treated cells, the apical delivery of apical residents was significantly impaired. Because both the rate and extent of their basolateral internalization were not significantly decreased, we propose that TGN to basolateral PM delivery was not impaired, i.e., the same amount of protein was synthesized and available for transcytosis. Similarly, VSV-G delivery from the TGN to the basolateral PM was not impaired in cholesterol-depleted Madin-Darby canine kidney (MDCK) cells (Keller and Simons, 1998). The internalization results also indicate that raft depletion specifically inhibits transcytotic efflux from basolateral early endosomes. This conclusion is consistent with the detection of intracellular populations of the transcytosing proteins in treated cells that colocalized with trafficked ASGP-R and partially overlapped with Tf-R. We suggest these structures are early endosomes, a common early transport intermediate of each of these molecules. A block at the early endosome also accounts for impaired pIgA-R transcytosis; it occurs downstream of clathrin-mediated uptake.

In contrast, endosomal trafficking of recycling receptors or HRP was not significantly affected by lipid depletion. Internalization of these markers was readily observed and their staining patterns were largely unchanged. The finding that Tf-R and ASGP-R remained partially colocalized in treated cells further implies Tf-R delivery to recycling endosomes via early endosomes was maintained. Based on studies performed in cholesterol-depleted Chinese hamster ovary cells where Tf-R recycling to the PM was unchanged (Subtil *et al.*, 1999), we further propose Tf-R recycled normally to the basolateral PM in lipid-depleted WIF-B cells.

Why was basolateral staining of most apical residents increased in treated cells when internalization was not impaired? Because there was no dramatic intracellular accumulation of internalized apical residents in treated cells, we propose that the apical residents rapidly recycled from the early endosome to the basolateral PM. Thus, normal TGN to basolateral delivery in combination with increased endosomal recycling would account for increased basolateral labeling. This is further substantiated by the finding that recycling, when assayed directly in Fao cells, was not significantly altered.

This model suggests that early endosomes contain raft domains. Although not tested directly, other intracellular populations of cholesterol have been identified. Recycling endosomes were found to be major storage compartments for cholesterol when the dynamics of fluorescently labeled cholesterol analogs were monitored (Mukherjee *et al.*, 1998). Immunoisolated recycling endosomes from polarized MDCK cells were also found to be enriched in SM and the raft-associated proteins caveolin and flotillin (Gagescu *et al.*, 2000). Late endosomes and lysosomes also have been shown to contain cholesterol, but to much lesser extents (Maxfield and Wustner, 2002).

The finding that basolateral internalization of apical proteins was not impaired in treated cells further suggests that rafts are not present at the basolateral PM or they do not mediate internalization of transcytosing apical proteins. The former possibility is consistent with results from experiments measuring fluorescence resonance energy between PM-associated raft markers where rafts were found to be at best a minor component of the cell surface (Kenworthy *et al.*, 2000). However, this contradicts reports from other studies indicating that 70–80% of the PM contains raft-like domains based on their solubility properties (Maxfield, 2002). Because other factors may also contribute to detergent insolubility (see below), this may be an overestimation. The possibility that raft depletion does not impair internalization has been suggested from experiments examining PM-to-Golgi delivery of ricin, lactosylceramide, and cholera toxin (Puri *et al.*, 1999; Rodal *et al.*, 1999; Shogomori and Futerman, 2001). In all cases, no decreases in internalization were observed. However, clathrin-mediated internalization of epidermal growth factor, transferrin, and Tf-R was severely impaired in cholesterol-depleted Chinese hamster ovary and Hep-2 cells where invagination of coated pits was perturbed (Rodal *et al.*, 1999; Shogomori and Futerman, 2001). Although we observed increased ASGP-R and Tf-R basolateral staining in treated WIF-B cells, the impairment of internalization was apparently mild given the intense intracellular labeling observed. This discrepancy may be explained by the different experimental conditions used. We had to use lower concentrations of mβCD (5 versus 10 mM in other studies) because WIF-B cells did not tolerate the higher doses (our unpublished data). Similarly, in hippocampal neurons treated with lower concentrations of mβCD, Tf-R internalization was not impaired (Shogomori and Futerman, 2001).

A General Component of the Transcytotic Trafficking Machinery Requires Raft Association

Why does depletion of raft components inhibit transcytosis from early endosomes? Findings that only a subset of the transcytosing proteins are detergent insoluble and that lipid depletion does not significantly alter their insolubility indicates that apical residents themselves do not require raft association for transcytotic sorting. Thus, we suggest that raft-dependent sorting is conferred by a general regulator of transcytosis whose activity requires raft association. One good candidate for this regulator is MAL2. The MAL family of raft-associated proteins are ~20-kDa tetra-spanning TMD proteins. Using an antisense approach, direct apical delivery was found to be decreased in MDCK cells lacking MAL; the ectopic expression of human MAL rescued the defect (Puertollano *et al.*, 1999; Martin-Belmonte *et al.*, 2000). Thus, MAL has been implicated as an important player in direct apical sorting. Interestingly, liver does not express this MAL isoform, a finding consistent with the absence of direct apical delivery of single-TMD and GPI-anchored apical residents in hepatocytes. Recently, another MAL isoform was identified, MAL2, that is enriched in hepatic cells (Wilson *et al.*, 2001; De Marco *et al.*, 2002). In HepG2 cells treated with antisense oligonucleotides, transcytosis of pIgA was blocked from early endosomes to what appeared to be the SAC (De Marco *et al.*, 2002). Thus, raft depletion may prevent MAL2 from sorting transcytosing proteins from early endosomes.

Another possible class of regulators is the soluble *N*-ethylmaleimide-sensitive factor attachment protein receptors (SNAREs). In both PC12 and MDCK cells, PM-associated t-SNAREs were detected in detergent-insoluble complexes (Lafont *et al.*, 1999; Chamberlain *et al.*, 2001). Confocal microscopic inspection of isolated PMs further revealed that t-SNAREs were present in clusters (Lang *et al.*, 2001). Cholesterol depletion dispersed the clusters and correlated with decreased exocytic activity (Chamberlain *et al.*, 2001; Lang *et al.*, 2001). Similarly, the apical SNAREs, syntaxin 3 and Ti-VAMP, were solubilized by mβCD in MDCK cells (Lafont *et al.*, 1999). These results suggest that the cholesterol-dependent organization of SNAREs is required for proper vesicle docking and fusion. If this organization is shared by SNAREs present on intracellular organelles, then the defect in transcytosis we observed might be explained by perturbed vesicle docking and fusion with the SAC or apical PM.

Why Do the Same Molecules Have Different Solubility Properties and What Imparts Detergent Insolubility?

The solubility properties of the apical residents presented in this study do not completely agree with other published determinations. For example, pIgA-R in intact enterocytes was ~50% insoluble, whereas it was completely soluble in WIF-B cells or FRT cells (Hansen *et al.*, 1999; Sarnataro *et al.*, 2000). Also, endogenous DPP IV is soluble in WIF-B, but partially insoluble in Fao cells, Caco-2 cells, and intact enterocytes (Danielsen, 1995; Alfalah *et al.*, 2002). There are several possible explanations for these disparate results. First, not all soluble and insoluble fractions are created equally. Many methods are cited for the preparation of detergent-insoluble domains. Perhaps the most prevalent one used includes a short, low-speed centrifugation (11,800 $\times$ *g* for 2 min). At the other extreme is a 30-min spin at 120,000 $\times$ *g*. When we tested these methods directly we found insolubility varied two- to threefold for APN and 5′NT (our unpublished data). Thus, it is important to note the methods used when making comparisons.

Perhaps a more interesting explanation for the differential solubility properties may reflect important differences in the cellular context. In particular, variations in membrane lipid composition may alter detergent insolubility. Similarly, these differences may also point to specialized mechanisms for protein sorting present in specific epithelial cell types. Are different MAL isoforms or SNAREs regulating specific protein sorting steps? Also important to consider are the different protein concentrations in different cell types. The more concentrated population of DPP IV at the Fao PM was more insoluble than in WIF-B cells. The reasons for this are

not clear, but this finding is important to consider when comparing results from different cell types.

What factors contribute to detergent insolubility? Although FB1 significantly decreased SM levels, all apical proteins tested maintained control insolubility levels. FB1 also failed to solubilize GPI-anchored proteins in FRT cells (Lipardi *et al*., 2000). Likewise, addition of mβCD did not alter the solubility of GPI-anchored proteins in Fao or WIF-B cells, of cholera toxin in T84 cells, or of galectin-4 in the intact enterocyte brush border (Hansen *et al*., 2001; Wolf *et al*., 2002). Simultaneous depletion of both lipid species still rendered 5′NT 50% insoluble. Although Triton X-100 insolubility was originally a diagnostic test for cytoskeletal association, the addition of cytochalasin D alone or in combination with mβCD failed to solubilize all apical residents (Figure 6; Brown and Rose, 1992). Thus, other unidentified factors are contributing to detergent insolubility. Alternatively, this result may reflect the uncertain relationship between rafts observed in vivo and detected in vitro.

Another Example of the Presence of Polarized Transport Pathways in Nonpolarized Cells

The results presented in this study add to the growing list of similarities between trafficking patterns in polarized and nonpolarized cells. Recently, we reported that like polarized cells, newly synthesized apical proteins in nonpolarized cells are delivered to the PM where they are selectively internalized and delivered to structures containing only other apical proteins (Tuma *et al*., 2002). Likewise, in both polarized and nonpolarized cells, raft depletion impairs trafficking of apical residents to these specific cellular destinations. However, in nonpolarized cells, these apical proteins normally recycle back to the PM, unlike their counterparts in fully polarized WIF-B cells where actin-dependent mechanisms normally prevent return. This recycling is not affected by raft depletion, leading to the disappearance of the apical compartment despite continuous internalization. Thus, the machinery required for specific intracellular sorting of apical residents is present in nonpolarized cells. Also striking was the observation that apical proteins in Fao cells had nearly identical solubility properties as in WIF-B cells. Together, these results indicate that raft-dependent sorting does not depend on the polarized state of a cell.

ACKNOWLEDGMENTS

We thank Drs. M. Farquhar, J.P. Luzio, and P. Morgan for generously providing antibodies. We also thank Dr. G. Ihrke for helpful comments about 5′NT solubilization and Dr. L. Leung for advice on the lipid analysis. We especially thank Dr. C. Machamer for providing instruction, reagents, and equipment for the TLC and for critically reading the manuscript. This work was supported by the National Institutes of Health grants GM-29185 and DK-44375 (to A.L.H.) and training grant DK-07632 (to P.L.T.).

REFERENCES

Alfalah, M., Jacob, R., and Naim, H.Y. (2002). Intestinal dipeptidyl peptidase IV is efficiently sorted to the apical membrane through the concerted action of *N*- and *O*-glycans as well as association with lipid microdomains. J. Biol. Chem. *277*, 10683–90.

Barr, V.A., and Hubbard, A.L. (1993). Newly synthesized hepatocyte plasma membrane proteins are transported in transcytotic vesicles in the bile duct-ligated rat. Gastroenterology *105*, 554–571.

Barr, V.A., Scott, L.J., and Hubbard, A.L. (1995). Immunoadsorption of hepatic vesicles carrying newly synthesized dipeptidyl peptidase IV and polymeric IgA receptor. J. Biol. Chem. *270*, 27834–27844.

Bartles, J.R., Braiterman, L.T., and Hubbard, A.L. (1985). Endogenous and exogenous domain markers of the rat hepatocyte plasma membrane. J. Cell Biol. *100*, 1126–1138.

Bartles, J.R., Feracci, H.M., Stieger, B., and Hubbard, A.L. (1987). Biogenesis of the rat hepatocyte plasma membrane in vivo: comparison of the pathways taken by apical and basolateral proteins using subcellular fractionation. J. Cell Biol. *105*, 1241–1251.

Bartles, J.R., and Hubbard, A.L. (1988). Plasma membrane protein sorting in epithelial cells: do secretory pathways hold the key? Trends Biochem. Sci. *13*, 181–184.

Bastaki, M., Braiterman, L.T., Johns, D.C., Chen, Y.H., and Hubbard, A.L. (2002). Absence of direct delivery for single transmembrane apical proteins or their "secretory" forms in polarized hepatic cells. Mol. Biol. Cell. *13*, 225–237.

Bligh, G.H., and Dyer, D.J. (1959). A rapid method of total lipid extraction and purification. Can. J. Biochem. Physiol. *37*, 911–917.

Brown, D.A., and Rose, J.K. (1992). Sorting of GPI-anchored proteins to glycolipid-enriched membrane subdomains during transport to the apical cell surface. Cell *68*, 533–544.

Brown, D.A., and London, E. (1998). Functions of lipid rafts in biological membranes. Annu. Rev. Cell. Dev. Biol. *14*, 111–136.

Cerneus, D.P., Ueffing, E., Posthuma, G., Strous, G.J., and van der Ende, A. (1993). Detergent insolubility of alkaline phosphatase during biosynthetic transport and endocytosis. Role of cholesterol. J. Biol. Chem. *268*, 3150–3155.

Chamberlain, L.H., Burgoyne, R.D., and Gould, G.W. (2001). SNARE proteins are highly enriched in lipid rafts in PC12 cells: implications for the spatial control of exocytosis. Proc. Natl. Acad. Sci. USA *98*, 5619–5624.

Danielsen, E.M. (1995). Involvement of detergent-insoluble complexes in the intracellular transport of intestinal brush border enzymes. Biochemistry *34*, 1596–605.

De Marco, M.C., Martin-Belmonte, F., Kremer, L., Albar, J.P., Correas, I., Vaerman, J.P., Marazuela, M., Byrne, J.A., and Alonso, M.A. (2002). MAL2, a novel raft protein of the MAL family, is an essential component of the machinery for transcytosis in hepatoma HepG2 cells. J. Cell Biol. *159*, 37–44.

Gagescu, R., Demaurex, N., Parton, R.G., Hunziker, W., Huber, L.A., and Gruenberg, J. (2000). The recycling endosome of Madin-Darby canine kidney cells is a mildly acidic compartment rich in raft components. Mol. Biol. Cell. *11*, 2775–2791.

Griffiths, G., Pfeiffer, S., Simons, K., and Matlin, K. (1985). Exit of newly synthesized membrane proteins from the trans cisterna of the Golgi complex to the plasma membrane. J. Cell Biol. *101*, 949–964.

Gu, F., Crump, C.M., and Thomas, G. (2001). trans-Golgi network sorting. Cell. Mol. Life Sci. *58*, 1067–1084.

Hansen, G.H., Immerdal, L., Thorsen, E., Niels-Christiansen, L.L., Nystrom, B.T., Demant, E.J., and Danielsen, E.M. (2001). Lipid rafts exist as stable cholesterol-independent microdomains in the brush border membrane of enterocytes. J. Biol. Chem. *276*, 32338–32344.

Hansen, G.H., Niels-Christiansen, L.L., Immerdal, L., Hunziker, W., Kenny, A.J., and Danielsen, E.M. (1999). Transcytosis of immunoglobulin A in the mouse enterocyte occurs through glycolipid raft- and rab17-containing compartments. Gastroenterology *116*, 610–622.

Harder, T., and Simons, K. (1997). Caveolae, DIGs, and the dynamics of sphingolipid-cholesterol microdomains. Curr. Opin. Cell Biol. *9*, 534–542.

Hubbard, A.L., Bartles, J.R., and Braiterman, L.T. (1985). Identification of rat hepatocyte plasma membrane proteins using monoclonal antibodies. J. Cell Biol. *100*, 1115–1125.

Ihrke, G., Martin, G.V., Shanks, M.R., Schrader, M., Schroer, T.A., and Hubbard, A.L. (1998). Apical plasma membrane proteins and endolyn-78 travel through a subapical compartment in polarized WIF-B hepatocytes. J. Cell Biol. *141*, 115–133.

Ihrke, G., Neufeld, E.B., Meads, T., Shanks, M.R., Cassio, D., Laurent, M., Schroer, T.A., Pagano, R.E., and Hubbard, A.L. (1993). WIF-B cells: an in vitro model for studies of hepatocyte polarity. J. Cell Biol. *123*, 1761–1775.

Ikonen, E., and Simons, K. (1998). Protein and lipid sorting from the trans-Golgi network to the plasma membrane in polarized cells. Semin. Cell. Dev. Biol. *9*, 503–509.

Keller, P., and Simons, K. (1998). Cholesterol is required for surface transport of influenza virus hemagglutinin. J. Cell Biol. *140*, 1357–1367.

Kenworthy, A.K., Petranova, N., and Edidin, M. (2000). High-resolution FRET microscopy of cholera toxin B-subunit and GPI-anchored proteins in cell plasma membranes. Mol. Biol. Cell *11*, 1645–1655.

Kilsdonk, E.P., Yancey, P.G., Stoudt, G.W., Bangerter, F.W., Johnson, W.J., Phillips, M.C., and Rothblat, G.H. (1995). Cellular cholesterol efflux mediated by cyclodextrins. J. Biol. Chem. *270*, 17250–17256.

Lafont, F., Verkade, P., Galli, T., Wimmer, C., Louvard, D., and Simons, K. (1999). Raft association of SNAP receptors acting in apical trafficking in Madin-Darby canine kidney cells. Proc. Natl. Acad. Sci. USA *96*, 3734–3738.

Lang, T., Bruns, D., Wenzel, D., Riedel, D., Holroyd, P., Thiele, C., and Jahn, R. (2001). SNAREs are concentrated in cholesterol-dependent clusters that define docking and fusion sites for exocytosis. EMBO J. *20*, 2202–2213.

Lipardi, C., Nitsch, L., and Zurzolo, C. (2000). Detergent-insoluble GPI-anchored proteins are apically sorted in Fischer rat thyroid cells, but interference with cholesterol or sphingolipids differentially affects detergent insolubility and apical sorting. Mol. Biol Cell *11*, 531–542.

Macala, L.J., Yu, R.K., and Ando, S. (1983). Analysis of brain lipids by high performance thin-layer chromatography and densitometry. J. Lipid Res. *24*, 1243–1250.

Martin-Belmonte, F., Puertollano, R., Millan, J., and Alonso, M.A. (2000). The MAL proteolipid is necessary for the overall apical delivery of membrane proteins in the polarized epithelial Madin-Darby canine kidney and Fischer rat thyroid cell lines. Mol. Biol. Cell. *11*, 2033–2045.

Matlin, K.S., and Simons, K. (1983). Reduced temperature prevents transfer of a membrane glycoprotein to the cell surface but does not prevent terminal glycosylation. Cell *34*, 233–243.

Maxfield, F.R. (2002). Plasma membrane microdomains. Curr. Opin. Cell Biol. *14*, 483–7.

Maxfield, F.R., and Wustner, D. (2002). Intracellular cholesterol transport. J. Clin. Investig. *110*, 891–898.

Mukherjee, S., Zha, X., Tabas, I., and Maxfield, F.R. (1998). Cholesterol distribution in living cells: fluorescence imaging using dehydroergosterol as a fluorescent cholesterol analog. Biophys. J. *75*, 1915–1925.

Ohtani, Y., Irie, T., Uekama, K., Fukunaga, K., and Pitha, J. (1989). Differential effects of alpha-, beta- and gamma-cyclodextrins on human erythrocytes. Eur. J. Biochem. *186*, 17–22.

Puertollano, R., Menendez, M., and Alonso, M.A. (1999). Incorporation of MAL, an integral protein element of the machinery for the glycolipid and cholesterol-mediated apical pathway of transport, into artificial membranes requires neither of these lipid species. Biochem. Biophys. Res. Commun. *266*, 330–333.

Puri, V., Watanabe, R., Dominguez, M., Sun, X., Wheatley, C.L., Marks, D.L., and Pagano, R.E. (1999). Cholesterol modulates membrane traffic along the endocytic pathway in sphingolipid-storage diseases. Nat. Cell Biol. *1*, 386–388.

Rodal, S.K., Skretting, G., Garred, O., Vilhardt, F., van Deurs, B., and Sandvig, K. (1999). Extraction of cholesterol with methyl-beta-cyclodextrin perturbs formation of clathrin-coated endocytic vesicles. Mol. Biol. Cell *10*, 961–974.

Saraste, J., Palade, G.E., and Farquhar, M.G. (1986). Temperature-sensitive steps in the transport of secretory proteins through the Golgi complex in exocrine pancreatic cells. Proc. Natl. Acad. Sci. USA *83*, 6425–6429.

Sarnataro, D., Nitsch, L., Hunziker, W., and Zurzolo, C. (2000). Detergent insoluble microdomains are not involved in transcytosis of polymeric Ig receptor in FRT and MDCK cells. Traffic *1*, 794–802.

Scheiffele, P., Peranen, J., and Simons, K. (1995). N-glycans as apical sorting signals in epithelial cells. Nature *378*, 96–98.

Scheiffele, P., Roth, M.G., and Simons, K. (1997). Interaction of influenza virus haemagglutinin with sphingolipid-cholesterol membrane domains via its transmembrane domain. EMBO J. *16*, 5501–5508.

Schell, M.J., Maurice, M., Stieger, B., and Hubbard, A.L. (1992). 5′nucleotidase is sorted to the apical domain of hepatocytes via an indirect route. J. Cell Biol. *119*, 1173–1182.

Shanks, M.S., Cassio, D., Lecoq, O., and Hubbard, A.H. (1994). An improved rat hepatoma hybrid cell line. Generation and comparison with its hepatoma relatives and hepatocytes in vivo. J. Cell Sci. *107*, 813–825.

Shogomori, H., and Futerman, A.H. (2001). Cholesterol depletion by methyl-beta-cyclodextrin blocks cholera toxin transport from endosomes to the Golgi apparatus in hippocampal neurons. J. Neurochem. *78*, 991–999.

Simons, K., and Ikonen, E. (1997). Functional rafts in cell membranes. Nature *387*, 569–572.

Subtil, A., Gaidarov, I., Kobylarz, K., Lampson, M.A., Keen, J.H., and McGraw, T.E. (1999). Acute cholesterol depletion inhibits clathrin-coated pit budding. Proc. Natl. Acad. Sci. USA *96*, 6775–6780.

Tuma, P., and Hubbard, A. (2001). The hepatocyte surface: dynamic polarity. In: The Liver: Biology and Pathology, ed. I. Arias, J. Boyer, F. Chisari, N. Fausto, D. Schachter, and D. Shafritz, Philadelphia: Lippincott Williams & Wilkins, 97–117.

Tuma, P., Nyasae, L., and Hubbard, A. (2002). Nonpolarized cells selectively sort apical proteins from cell surface to a novel compartment, but lack apical retention mechanisms. Mol. Biol. Cell *13*, 3400–3415.

Wall, D.A., and Hubbard, A.L. (1985). Receptor-mediated endocytosis of asialoglycoproteins by rat liver hepatocytes: biochemical characterization of the endosomal compartments. J. Cell Biol. *101*, 2104–2112.

Wilson, S.H., Bailey, A.M., Nourse, C.R., Mattei, M.G., and Byrne, J.A. (2001). Identification of MAL2, a novel member of the mal proteolipid family, though interactions with TPD52-like proteins in the yeast two-hybrid system. Genomics *76*, 81–88.

Wolf, A.A., Fujinaga, Y., and Lencer, W.I. (2002). Uncoupling of the cholera toxin-G(M1) ganglioside receptor complex from endocytosis, retrograde Golgi trafficking, and downstream signal transduction by depletion of membrane cholesterol. J. Biol. Chem. *277*, 16249–16256.